Biochemistry

 Volume 37, Number 36 September 8, 1998

Accelerated Publications

NMR-Based Model of a Telomerase-Inhibiting Compound Bound to G-Quadruplex DNA†

Oleg Yu. Fedoroff,*,‡ Miguel Salazar,§,|| Haiyong Han,|| Violetta V. Chemeris,‡ Sean M. Kerwin,*,§,|| and Laurence H. Hurley*,‡,||

Drug Dynamics Institute, College of Pharmacy, Division of Medicinal Chemistry, and Program in Molecular Biology, The University of Texas at Austin, Austin, Texas 78712

Received June 5, 1998; Revised Manuscript Received July 13, 1998

ABSTRACT: The single-stranded $(TTAGGG)_n$ tail of human telomeric DNA is known to form stable G-quadruplex structures. Optimal telomerase activity requires the nonfolded single-stranded form of the primer, and stabilization of the G-quadruplex form is known to interfere with telomerase binding. We have identified 3,4,9,10-perylenetetracarboxylic diimide-based ligands as potent inhibitors of human telomerase by using a primer extension assay that does not use PCR-based amplification of the telomerase primer extension products. A set of NMR titrations of the ligand into solutions of G-quadruplexes using various oligonucleotides related to human telomeric DNA showed strong and specific binding of the ligand to the G-quadruplex. The exchange rate between bound and free DNA forms is slow on the NMR time scale and allows the unequivocal determination of the binding site and mode of binding. In the case of the 5′-TTAGGG sequence, the ligand−DNA complex consists of two quadruplexes oriented in a tail-to-tail manner with the ligand sandwiched between terminal G4 planes. Longer telomeric sequences, such as TTAGGGTT, TTAGGGTTA, and TAGGGTTA, form 1:1 ligand−quadruplex complexes with the ligand bound at the GT step by a threading intercalation mode. On the basis of 2D NOESY data, a model of the latter complex has been derived that is consistent with the available experimental data. The determination of the solution structure of this telomerase inhibitor bound to telomeric quadruplex DNA should help in the design of new anticancer agents with a unique and novel mechanism of action.

Telomeres are important multifunctional nucleoprotein structures found at the ends of eukaryotic chromosomes. They ensure the complete replication of chromosomal DNA and protect the chromosome ends from fusion and degradation (reviewed in refs *1* and *2*). In vertebrates, telomeric DNA contains a double-stranded region made from the simple repeat sequence TTAGGG and a single-stranded 3′-end overhang (*3*). The single-stranded tail of human telomeres is surprisingly long, averaging more than 150 bases in length, and may be involved in controlling telomerase activity and telomere to telomere interactions (*4*, *5*). Telomeres of human somatic cells have 1000−3000 repeats and gradually shorten with every cell division (*6*, *7*). This shortening serves as a mitotic clock that appears to limit the proliferative capacity of somatic cells (*8*). In contrast, immortal cancer cells have an unlimited proliferative poten-

† This work was supported by a grant from the National Institutes of Health (CA-49751) and a National Cooperative Drug Discovery Group grant (CA-67760).

* Address correspondence to these authors.
‡ Drug Dynamics Institute, College of Pharmacy.
§ Division of Medicinal Chemistry.
|| Program in Molecular Biology.

S0006-2960(98)01330-0 CCC: $15.00
Published on Web 08/15/1998

Scheme 1

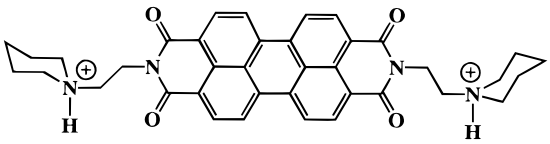

tial, and as a prerequisite, they must maintain stable telomeric length (*3*, *6*). The major mechanism of telomere length maintenance is the reactivation of telomerase, a specific reverse transcriptase with an endogenous RNA template (*9*−*11*). A high level of telomerase activity has been associated with cancer cells and may be essential for their immortality. Therefore, telomerase, and in a broader sense, the telomere itself, has been proposed as a potential chemotherapeutic target for noncytotoxic anticancer agents (*11*−*14*).

A detailed three-dimensional structure of telomerase is unknown, but structural precedent and all the available experimental data point to normal Watson−Crick pairing between the DNA primer and RNA template in the core of the elongated telomerase complex (*11*, *15*). Thus, the optimal conformation of the primer substrate should be the unfolded single-stranded DNA with all functional groups available for template binding. However, the single-stranded guanine-rich DNA molecules are well-known to form a variety of G-quadruplex structures, with $(TTAGGG)_n$ being no exception (*16*−*18*). Stabilization of folded G-quadruplex structures in telomeric sequences has been shown to interfere with telomerase activity (*19*) and is a new paradigm for anticancer drug development (*14*).

Telomeres are not the only DNA segments in the human genome that have been shown to form G-quadruplex structures *in vitro*, and possibly *in vivo*. G-quadruplex structures have been implicated in the mechanism of Ig class switch recombination (*20*) and regulation of transcriptional activity of some promoters (*21*−*23*). Moreover, a variety of proteins bind to quadruplex DNA with high affinity and specificity (for a recent review, see ref *24*). G4 DNA can also serve as a substrate for DNA topoisomerase II (*25*), Xrn1p/Kem1 nuclease (*26*, *27*), and other enzymes involved in DNA metabolism (*28*). The emerging evidence for the functional biological role of G4 DNA begs for the identification and development of new low molecular weight ligands specific for G-quadruplex structures. Such ligands might be useful for studying the biological role of G-quadruplexes and may serve as leads for the development of a new class of antiproliferative therapeutic drugs. Several studies have reported the spectroscopic investigations of drug interactions with G-quadruplexes, but no definite structural information has been so far available (*14*, *28*−*32*). Here we present structural studies of parallel G-quadruplex binding by the telomerase-inhibiting compound *N*,*N*′-bis[2-(1-piperidino)-ethyl]-3,4,9,10-perylenetetracarboxylic diimide (hereafter abbreviated PIPER) (Scheme 1).

MATERIALS AND METHODS

Sample Preparations. *N*,*N*′-Bis[2-(1-piperidino)ethyl]-3,4,9,10-perylenetetracarboxylic diimide (PIPER) was synthesized and purified following the published procedure (*33*). Three grams of 3,4,9,10-perylenetetracarboxylic dianhyride was mixed with 2.5 mL of 1-(2-aminoethyl)piperidine in 10 mL of DMA and 10 mL of 1,4-dioxane. The mixture was heated under reflux for 6 h, and the solvents were removed under reduced pressure. The residue was dissolved in 100 mL of distilled water, and insoluble components were removed by filtration. The pH of the resulting solution was adjusted to ∼3 with the addition of HCl, and the solution was allowed to stand overnight. Precipitated impurities were removed by filtration, and the resulting solution was adjusted to pH 12 with the addition of NaOH. The precipitated product was isolated by filtration, washed with deionized water, dried under vacuum, and characterized by ^{1}H NMR and high-resolution chemical ionization mass spectrometry.

DNA oligonucleotides were synthesized on a 15 μM scale on a Perseptive Biosystems Expedite 8909 automatic DNA synthesizer, purified by reverse-phase HPLC on a C18 column (Dynamax-300A), and dialyzed extensively, first against 10 mM KCl solution and then against deionized water. Solid supports and phosphoramidites were purchased from Glen Research and Perseptive Biosystems.

NMR Spectroscopy. NMR experiments were performed on a Varian UNITYplus 500 MHz spectrometer. All titration experiments were carried out at 30 °C in a 90% H_2O/10% D_2O solution containing 150 mM KCl, 25 mM KH_2PO_4, and 1 mM EDTA (pH 7.0). A standard 1−1 echo pulse sequence with a maximum excitation centered at 12.0 ppm was used for water suppression. Thirty-two scans were acquired for each spectrum with a relaxation delay of 2 s. 2D NOESY spectra of exchangeable protons were collected at 35 and 50 °C in TPPI mode with a mixing time of 200 ms using 2048 complex points in t_2 and 1024 t_1 experiments. One known feature of G-quadruplex DNA is a very slow exchange rate of imino protons involved in tetrad formation (*16*). Even at 50 °C, all guanine imino protons had narrow line widths and were easily assigned following the published assignment procedure for parallel quadruplexes (*16*, *39*). NOESY and DQF-COSY spectra of nonexchangeble protons were collected at 50 °C in a phase-sensitive mode using 2048 complex points in t_2 and 512 pairs of real and imaginary t_1 experiments. Four mixing times of 100, 200, 300, and 400 ms were used in the NOESY experiments. NMR data were processed and analyzed using the FELIX program (Molecular Simulations, Inc.). Nearly all nonexchangeble DNA protons of the $[dTTAGGG]_4$ and $[dTAGGGTTA]_4$ complexes, except for several H5′/H5″ pairs, were assigned by routine sequential assignment procedures (*16*, *39*). Assignments were verified by monitoring exchange peaks between protons of free and complexed DNA in the NOESY spectrum of a partially titrated sample (not shown). The studied oligonucleotides do not contain any cytosine residues, and the aromatic protons of PIPER could be easily assigned as the only protons producing a COSY cross-peak in the downfield spectral region. Taking these protons as a starting point, the remaining drug protons were assigned by analyzing NOESY and COSY spectra. Assignments of piperidine ring protons were nonstereospecific.

Model Building and Molecular Dynamics Refinement. The starting structure for molecular modeling of PIPER−quadruplex complexes was the published crystal structure of the parallel quadruplex TGGGGT (PDB entry 244d) (*40*). The necessary replacements and additions of residues were carried out using the INSIGHTII program (Molecular Simulations, Inc.). Restrained molecular dynamics (10 ps at 250 K) and mechanics (2000 cycles conjugated gradient minimization)

were subsequently used for energy refinement of the models (DISCOVER program with AMBER force field, Molecular Simulations, Inc.). After initial refinement of the free DNA structure, the drug molecule was manually placed in the proposed binding site. The PIPER−DNA complex model was subjected to a combination of restrained molecular dynamics (20 ps at 250 K) and conjugate gradient refinement. Twenty independent runs were performed for better sampling of conformational space. The distance restraints were taken from build-up curves of NOESY cross-peaks and assigned as either strong (2.0−2.8 Å), medium (2.5−4.0 Å), or weak (3.5−5.5 Å). The intensities of the H1′−H2′ cross-peaks were used as reference peaks, since the H1′−H2′ distances of the deoxyribose ring are largely independent of the sugar conformation (2.1−2.2 Å range). The isolated spin approximation was used to estimate distances. The obtained values were then extrapolated to 0 ms mixing time to take into account spin diffusion. No attempts were made to employ the relaxation matrix refinement. Any attempts to derive distance restraints more accurately could produce misleading and potentially biased results due to the highly dynamic nature of the PIPER−quadruplex complexes (see later).

Circular Dichroism Spectra. Spectra were recorded on a Jasco J600 spectropolarimeter. The same buffer was used as for NMR spectroscopy. Experiments were performed at 20 °C in a 0.5 cm path length cell.

Telomerase Assay. The assay was performed by using 5′-end biotinylated d[TTAGGG]$_3$ as the telomere primer (*14*). Reaction mixtures (20 μL) containing 5 L of cell lysate (S-100), 50 mM Tris−OAc (pH 8.5), 50 mM KOAc, 1 mM $MgCl_2$, 5 mM BME, 1 mM spermidine, 1 μM telomere primer, 1.5 μM [α-^{32}P]dGTP (800 Ci/mmol), 1 mM dATP, and 1 mM dTTP were incubated at 37 °C for 1 h, and the reactions were terminated by addition of 20 μL of a [^{32}P]-ATP-labeled streptavidin-coated Dynabeads suspension containing 10 mM Tris-HCl (pH 7.5), 1 mM EDTA, 2 M KCl, and a 500 cpm biotinylated internal control. Streptavidin-coated Dynabeads bind selectively to the desired target (5′-biotinylated primer), forming a magnetic bead-targeted complex. The complex was separated from the suspension using a Dynal MPC magnet and washed several times with 2× SSC buffer containing 0.1% SDS to eliminate [α-^{32}P]-dGTP background. Telomerase reaction products were separated from the magnetic beads by protein denaturation with 5.7 M guanidine hydrochloride at 90 °C for 30 min. After ethanol precipitation, products were resolved on denaturing 10% polyacrylamide gel.

DNA Synthesis Arrest Assay. The assay was a modification of the procedure described by Weitzmann and coworkers (*33*). Briefly, primers (24 nM) labeled with [γ-^{32}P]ATP were mixed with template DNA [5′-TCCAAC-TATGTATAC(TTGGGG)$_4$TTAGCGGCACGCAATTGC-TATAGTGAGTCGTATTA-3′] in a Tris-HCl buffer (10 mM Tris, pH 8.0) containing 10 mM $MgCl_2$ and heated at 90 °C for 4 min. After the solution was cooled at room temperature for 15 min, PIPER was added at the concentrations indicated in Figure 6B. The primer extension reactions were initiated by addition of dNTP (final concentration, 100 μM) and Taq DNA polymerase (2.5 unit/reaction, Boehringer Mannheim). The reactions were performed at 55 °C for 15 min and then stopped by addition of an equal volume of stop buffer (95%

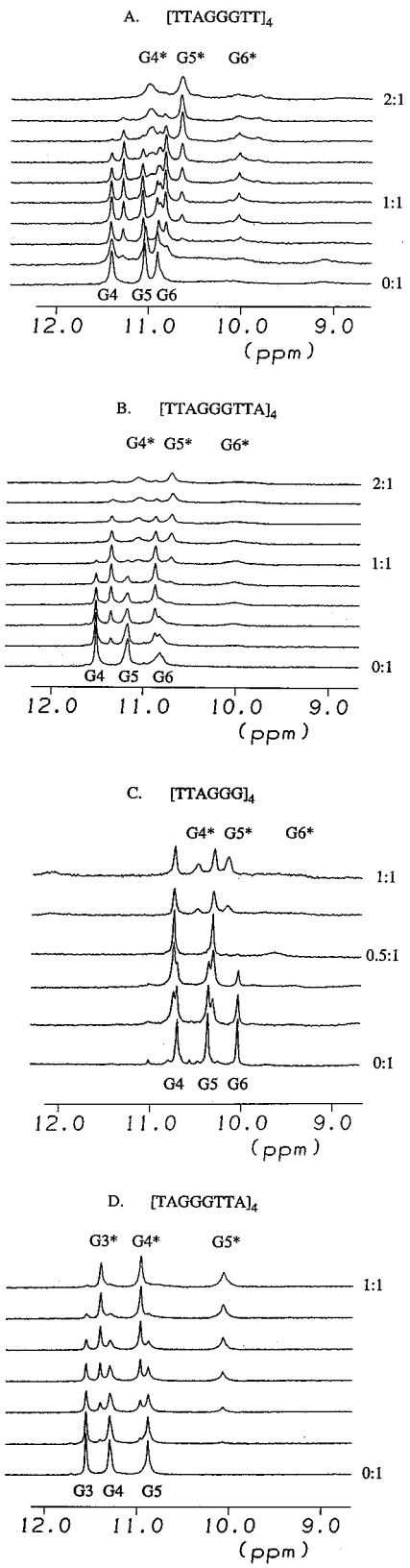

FIGURE 1: Titration of (A) [dTTAGGGTT]$_4$, (B) [dTTAGGGTTA]$_4$, (C) [dTTAGGG]$_4$, and (D) [dTAGGGTTA]$_4$ with PIPER. The imino proton region of the 500 MHz NMR is shown with increasing amounts of ligand added at 30 °C. In (A−C) G4, G5, and G6 label the original imino proton resonances that disappear from the spectra with increasing amounts of ligand. G4*, G5*, and G6* represent resonances of the final ligand−quadruplex complexes. The corresponding labeling of imino protons in (D) is G3, G4, and G5.

formamide, 10 mM EDTA, 10 mM NaOH, 0.1% xylene cyanol, 0.1% bromophenol blue). The products were separated on a 12% polyacrylamide sequencing gel.

RESULTS AND DISCUSSION

Complex Formation and Stoichiometry. The choice of DNA sequences for the present study was dictated by our motivation to discover compounds that will selectively inhibit human telomerase by targeting unique telomeric DNA structures, especially G-quadruplexes. $(TTAGGG)_n$ can form both intermolecular (*16*) and intramolecular complexes (*17*), depending on sequence length and environment (*18*). Intermolecular-type structures might have less biological relevance than an intramolecular foldover G-quadruplex, although they have been proposed to occur *in vivo* in recombination, telomere pairing, etc. The NMR spectra of the intramolecular G-quadruplex formed by d[(AGGG)d-$(TTAGGG)_3$] are quite complex (*17*). Moreover, long human telomeric sequences with more than one GGG block usually exist in equilibrium involving several folded forms with different topology and intermolecular aggregates of ill-defined sizes (data not shown). This has made it difficult to interpret the ligand−intramolecular G-quadruplex interactions by NMR, which is why we concentrated on studying much simpler intermolecular G-quadruplex structures formed by shorter oligonucleotides such as TTAGGG and TAGGGTTA. Nevertheless, UV and NMR titration experiments (results not shown) indicate that PIPER also interacts with a foldover intramolecular quadruplex, although a detailed structural characterization has so far been unsuccessful.

The 1D NMR spectra recorded during the titration of $[dTTAGGGTT]_4$ with PIPER are shown in Figure 1A. The original NMR signals of Hoogsteen-bound guanine imino protons (10−12 ppm range) gradually disappear during the titration, and a new set of reciprocal upfield-shifted imino proton resonances appears. Separate proton resonances for the free DNA and the PIPER−DNA complex indicate slow exchange on the NMR time scale between free and bound states, which is usually interpreted as an indication of tight and specific binding. Surprisingly, at a 1:1 ligand:quadruplex stoichiometry, another set of new proton signals can be observed, which become dominant with increasing drug concentration. Continuous titration to a 2:1 ligand:DNA ratio results in the total disappearance of both the original and first set of new signals. Further titration beyond this point led only to broadening of the proton resonances without any substantial changes in the spectrum. The most logical explanation for the observed behavior is the presence of two drug binding sites with slightly different affinities. At a low ligand to DNA ratio, ligand molecules first occupy the strongest binding site. However, if the binding affinities of the first and second binding sites are of the same order of magnitude, the principle of mass action would dictate that at a higher ligand concentration the binding to the second site would become detectable even before the binding to the first site is saturated.

Reliable structural determination by ^{1}H NMR requires the presence of a single, well-defined structure in solution with relatively narrow proton resonances. The spectra of the PIPER−$[dTTAGGGTT]_4$ complex were found unsuitable for this purpose. Therefore, other G-quadruplex-forming oligonucleotides were evaluated. From a comparison of the titration spectra, it appears that the relative affinities of two putative binding sites can be modified by varying the length of 5′- and 3′-overhangs. For example, titration of $[dTTAGGGTTA]_4$ produces a cleaner NMR spectrum at a 1:1 PIPER:DNA ratio, with a much smaller fraction of the 2:1 complex (Figure 1B). Among the eight sequences we tested, only the drug complexes with the $[dTTAGGG]_4$ and $[dTAGGGTTA]_4$ quadruplexes produced simple spectra with a single species in solution (Figure 1C,D). However, while the expected 1:1 ligand−quadruplex complex is formed with $[dTAGGGTTA]_4$, a 1:2 ligand−quadruplex complex is formed with $[dTTAGGG]_4$, since there were no detectable free $[dTTAGGG]_4$ molecules at a 0.5:1 ligand:DNA ratio. The recurrent spectral feature of all studied ligand−quadruplex complexes is a severe line broadening of the imino proton of the last guanine (G5 in $[dTAGGGTTA]_4$ and G6 in $[dTTAGGG]_4$), indicating that PIPER binds near this site.

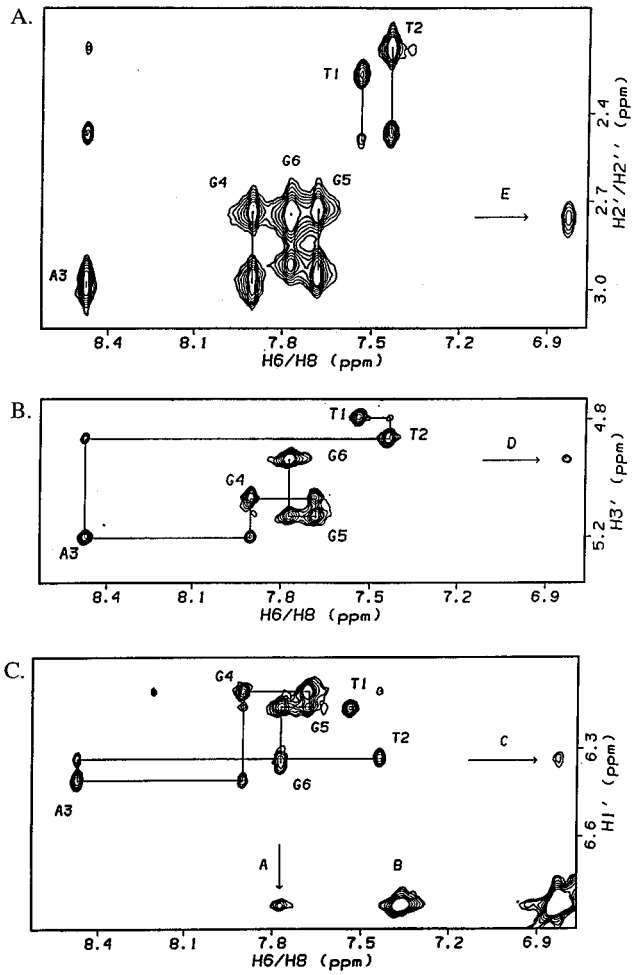

FIGURE 2: Sections of the 2D NOESY spectrum of the 2:1 [dTTAGGG]$_4$−PIPER complex at 50 °C. (A) H6/H8−H2′/H2″ spectral region with intraresidue cross-peaks connected by vertical lines. H2″ peaks are labeled with residue numbers. G6 H2′ and H2″ have identical chemical shifts, and peak E is an intermolecular cross-peak between either of these protons and the ligand. (B) Assignment of DNA H6/H8−H3′ protons. Peak D is an intermolecular cross-peak between G6 H3′ and the ligand. (C) Sequential walk assignment of the DNA H6/H8−H1′ protons. Intrastrand peaks are labeled with residue numbers. Peaks A and C are intermolecular NOEs between the ligand and G6 H8 and H1′ protons, respectively. Peak B is an intramolecular cross-peak between aromatic protons of the ligand.

Scheme 2

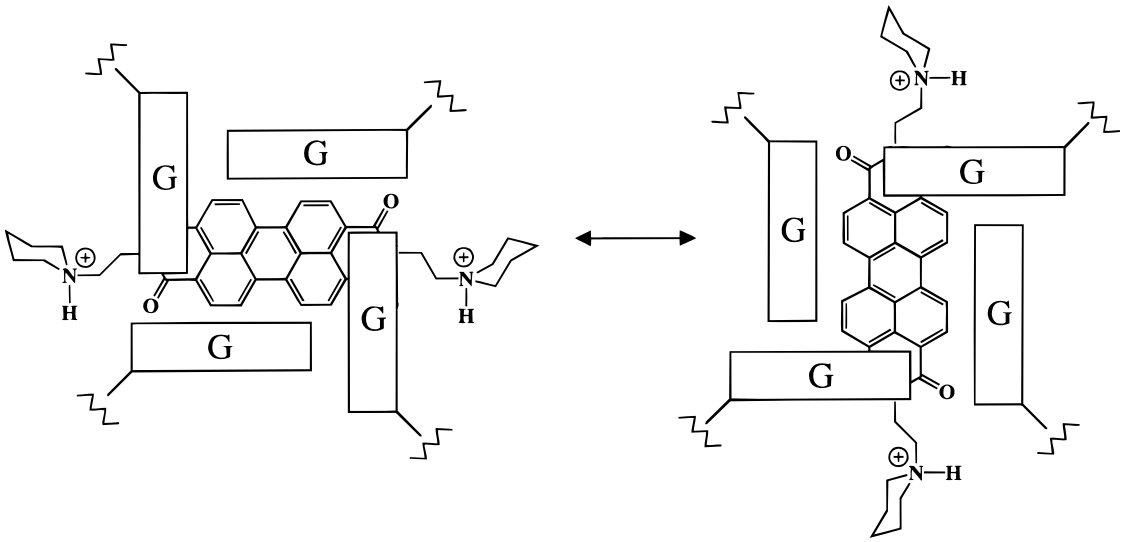

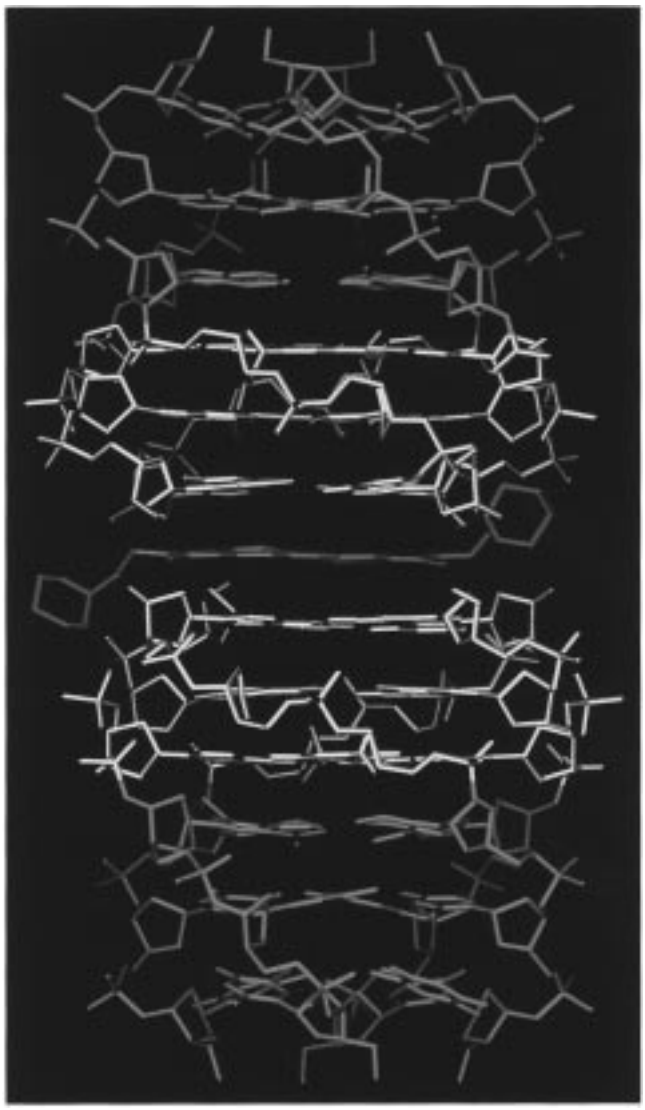

FIGURE 3: NMR-based model of the 2:1 $[dTTAGGG]_4$−PIPER complex. The ligand molecule is sandwiched between two G6 guanine tetrads with positively charged side chains located in the grooves. Guanine residues are in yellow, thymine and adenine are in purple, and the ligand molecule is in green. The interproton distances corresponding to intermolecular cross-peaks shown in Figure 2 are in the 2.5−4.5 Å range.

This peak sharpens with increasing temperature, indicating the dynamic nature of the PIPER−DNA complex (see later). As with any positively charged ligand, PIPER is capable of binding nonspecifically to nucleic acids (*33*). However, this binding is apparently much weaker than binding to G-quadruplexes since titration of PIPER into solutions of several double-stranded DNA oligonucleotides produced only general peak broadening at high drug concentration, with no resemblance to the spectral changes observed with the G-quadruplex samples (data not shown).

$[dTTAGGG]_4$ Forms a Stable Tail-to-Tail Quadruplex−Ligand−Quadruplex Complex. 2D NMR spectra at the 1:2 PIPER:DNA titration point were collected at 50 °C and used for structure determination. The standard sequential DNA connectivities can be traced between aromatic and sugar protons (H1′, H2′/2″, and H3′) (Figure 2). Moreover, when the spectra of free DNA and the ligand−DNA complex are compared, drug binding shows little if any effect on the intensities of almost all DNA intra- and interresidue NOE cross-peaks. Thus, the structure of the DNA quadruplex in the complex appears to be virtually identical to the structure of the free DNA quadruplex, with all residues in the anti conformation with standard backbone geometry (*16*). Drug binding causes perturbations in the chemical shifts of the G6 protons, and most importantly, it results in the appearance of intermolecular NOE cross-peaks between ligand and DNA. All observed PIPER−DNA NOEs were assigned to G6 protons only (Figure 2). Thus, the most reasonable model that can explain the NMR data is a sandwich-type complex, with the ligand molecule stacked between the planes of terminal G6 tetrads (Figure 3). This model is consistent with all observed NOEs and explains the 1:2 PIPER:DNA stoichiometry. The strong $\pi-\pi$ stacking between two guanine tetrads and the drug chromophore is likely to be the major energetic factor in stabilizing the ligand−bis−quadruplex complex. Further support for this model is the fact that the drug-free $[dTTAGGG]_4$ *already* exists as a back-to-back dimer in solution (*16*). The dimeric form of G-quadruplexes with a blunt-ended guanine motif at the 3′-end is a dominant form at high salt concentrations (more than 50 mM KCl) and is characterized by a strong upfield shift of imino protons in comparison with 3′-extended

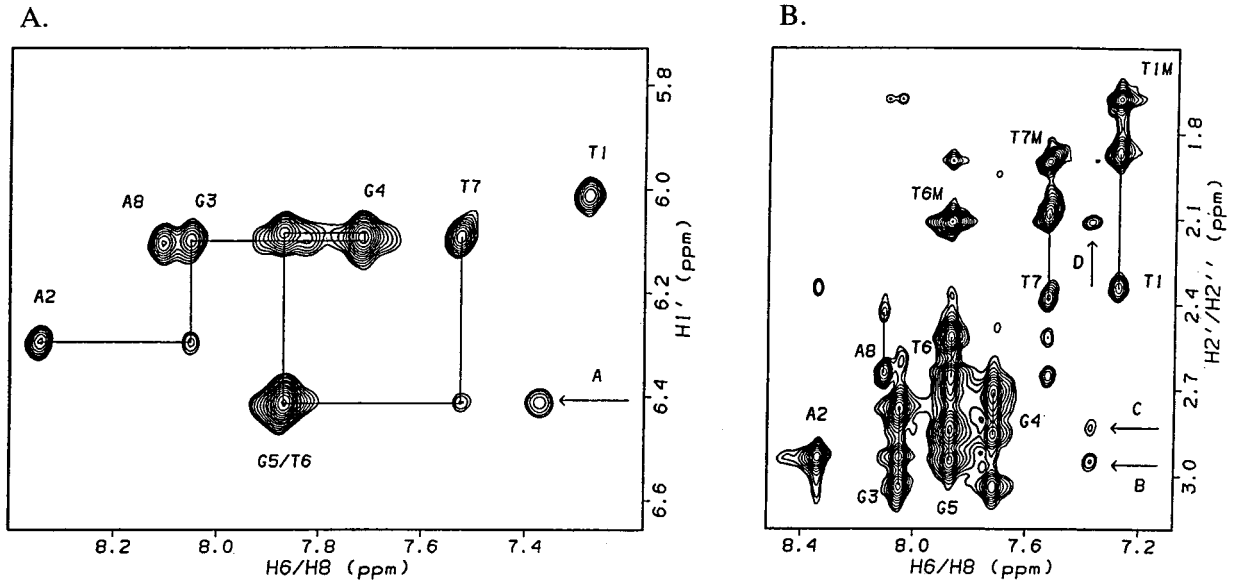

FIGURE 4: Sections of the 2D NOESY spectrum of the 1:1 $[dTAGGGTTA]_4$−PIPER complex at 50 °C. (A) Sequential walk assignment of the DNA H6/H8−H1′ protons. Intrastrand peaks are labeled with residue numbers. Peak A is an intermolecular NOE between the ligand and either of the overlapping G5 H1′ or T6 H1′ protons. (B) H6/H8−H2′/H2″/TMe spectral region with intraresidue cross-peaks connected by vertical lines. H2″ peaks are labeled with residue numbers. Peaks B, C, and D are intermolecular NOEs between the ligand and G5 H2″, H2′, and T6Me, respectively.

G-quadruplex sequences (*16*). Indeed, the chemical shifts of upfield-shifted imino protons of $[dTTAGGG]_4$ in our sample (compare Figure 1C with Figure 1A,B,D) correspond to assignments of the dimer rather than the monomer (*16*).

The parallel G-quadruplex DNA has C_4 symmetry, with all four strands being equal, while the ligand molecule has only C_2 symmetry. Since half of the guanine bases would be oriented parallel and half would be orthogonal with respect to the drug molecule (Scheme 2 and Figure 3), we might expect a doubling of at least some resonances upon drug binding. However, only a single set of resonances was observed in the NMR spectra (Figures 1 and 2), indicating a fast reorientation of the bound drug molecule on the NMR time scale. NMR signals broaden significantly at lower temperatures and sharpen with increasing temperature, with the G6 protons being the most affected, which is also consistent with both the binding site localization and the dynamic nature of the ligand−quadruplex complex.

PIPER Binds to [dTAGGGTTA]$_4$ at the GT Step by a Threading Intercalation Mode. Assuming parallel G-quadruplexes actually exist *in vivo*, they would most likely contain 3′-overhang sequences, decreasing the relevance of the blunt-ended $[dTTAGGG]_4$ as a model system. Among the ligand−quadruplex complexes that we studied, the best quality NMR spectra were obtained for $[dTAGGGTTA]_4$. This sequence was chosen for detailed structural studies even though the similarity in chemical shift changes suggests an identical binding mode for all studied parallel quadruplexes, regardless of the exact length of the 5′- and 3′-overhangs. 2D NMR spectra of the 1:1 ligand−quadruplex complex were collected at 50 °C. Inspection of the NOESY spectra revealed intermolecular NOEs between ligand protons and protons of G5 (the third guanine in the GGG block) and T6 (see Figure 4). As for the TTAGGG sequence, the structure of the actual $[GGG]_4$ quadruplex core remains unperturbed by ligand binding since the intensities of the observed intraresidue NOEs are virtually unchanged. Thus, the ligand

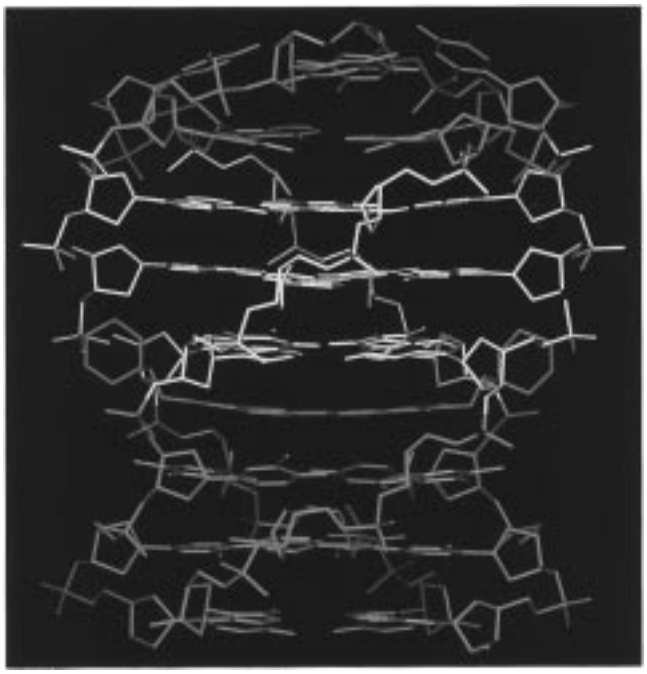

FIGURE 5: NMR-based model of the 1:1 $[dTAGGGTTA]_4$−PIPER complex. The ligand molecule is in blue, the DNA guanine residues are in yellow, and the adenine and thymine residues are in purple. The interproton distances corresponding to intermolecular cross-peaks shown in Figure 4 are in the 2.0−5.0 Å range.

molecule does not intercalate within the G-quadruplex itself but rather stacks on the surface of the 3′-terminal G-tetrad. This binding mode can be classified as a threading intercalation in the case of G-quadruplexes with 3′-overhang sequences, and as in the case of the $[dTTAGGG]_4$−PIPER complex, the single set of proton resonances implies a fast structural transition between the two orthogonal drug orientations. Thymine imino protons were not detected for either the free or ligand-bound DNA at temperatures higher than 10 °C. Moreover, the sequential NOEs in the TTA tail are

all very weak, implying weak stacking interactions. Apparently, the structure of the TTA tail is relatively loose and does not significantly impede the reorientation of the ligand. The structural transitions inside the complex are fast on the NMR time scale and should occur without drug disassociation from the complex. This is evident from the much slower exchange between ligand-bound and free DNA observed during titration and from the 2D NOESY spectra of partially titrated samples (data not shown).

The highly dynamic nature of the ligand−quadruplex complex makes the precise structural characterization extremely difficult. Each ligand−DNA cross-peak results from NOEs between ligand and both parallel and perpendicularly oriented DNA bases (Scheme 2). Therefore, the cross-peak intensity cannot be traced accurately to a particular interproton distance. Thus, we resorted to using very conservative distance restraints in order to avoid artifacts during molecular modeling. Due to this limitation, the precise structure (in terms of rmsd and NOE *R*-factor) cannot be determined; nevertheless, the proposed model (Figure 5) is accurate within its limitations and explains all the available experimental data. Additional structural information can be obtained from the circular dichroism (CD) spectrum. Like many other small molecular weight ligands, PIPER is an achiral molecule and does not have an intrinsic CD spectra. However, upon binding to DNA, a weakly induced CD signal for PIPER can be detected (data not shown). The signal follows the shape of the UV absorbance curve, indicating a nondegenerative dipole coupling mechanism (*31*). The observed weak intensity of the induced CD is typical for DNA intercalators and rules out the groove binding mode, which should result in a signal at least an order of magnitude stronger (*33*). Even at a high ligand concentration, we did not detect the exiton-coupled CD spectra of the ligand chromophore. This may indicate a significant spatial separation between bound ligand molecules (*31*). According to the NMR data, the strongest binding site for PIPER is the 3′-boundary of the G-quadruplex. Among the guanine imino protons, the proton of the 3′-terminal guanine is the most affected upon ligand binding, followed by a smaller chemical shift change of the central guanine imino proton, with the 5′-guanine being affected the least. The binding of a second ligand molecule is characterized by a reverse in the order of chemical shift changes: the chemical shift of the 5′-guanine imino proton changes most, while the chemical shift of the 3′-end guanine imino proton is almost unaffected by the binding of a second ligand molecule (Figure 1). Therefore, we propose that the second molecule binds at the opposite end of the guanine quadruplex, i.e., at the "top" (5′-end) of the G-tetrad block. The apparent weaker affinity of the secondary binding site can be attributed to a stronger stacking of the AG step at the 5′-end of the quadruplex, compared to GT stacking at the 3′-end. This localization of the binding sites is also consistent with the fact that we can manipulate their relative binding affinities simply by changing the lengths of the 3′- *or* 5′-overhangs (Figure 1). The G-quadruplex is an extremely stable and rigid structure, and distortion of quadruplex integrity, necessary for intercalator binding between G-tetrads inside the quadruplex, should involve a very high energy cost. Thus, stacking of the drug on the outer planes of G-tetrads appears to be an energetically more attractive alternative and may be a paradigm for quadruplex binding, not only for perylene-based compounds but for other molecules with G-quadruplex DNA intercalation potential (*14*, *32*).

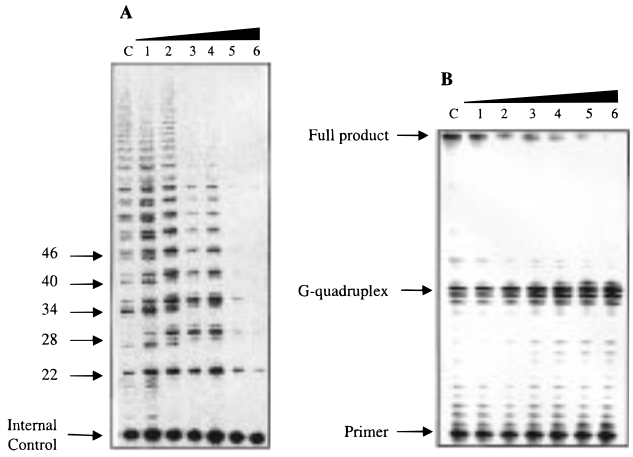

FIGURE 6: (A) Effect of increasing concentrations of PIPER on the inhibition of telomerase-catalyzed extension of a d[TTAGGG]$_3$ primer (1 μM concentration). Lane C is the control (no ligand added), and lanes 1−6 are the products of the telomerase reaction in the presence of 0, 5, 20, 50, 75, and 100 μM ligand. The numbers to the left of the gel refer to the telomerase extensions (in bases). (B) Effect of increasing concentrations of PIPER on inhibition of Taq polymerase DNA synthesis. Lane C is the control (no ligand added), and lanes 1−6 are the products of the reaction in the presence of 0.1, 0.5, 1, 2, 5, and 10 μM ligand. The arrows indicate the sites of full product, G-quadruplex formation on the DNA template, and primer.

Biochemical Effects of PIPER Binding to the DNA Quadruplex. Recently, our laboratory identified several G-quadruplex-interactive compounds as potent telomerase inhibitors (*14*, *32*). PIPER also shows good telomerase inhibition activity in a standard primer extension assay that does not use the PCR-based amplification of the telomerase primer extension products (Figure 6A). Interestingly, at low micromolar concentrations, PIPER has no effect on the first several rounds of telomeric repeat addition but inhibits telomerase activity when the product length reaches a certain point, in accordance with our previous results with a 2,6-disubstituted anthraquinone (*14*) and a porphyrin (*32*). It is tempting to speculate that longer TTAGGG repeats have a higher propensity to form G-quadruplex structures, which upon binding by PIPER are poor substrates for telomerase.

It has been shown that DNA sequences with quadruplex-forming potential present obstacles to DNA synthesis by DNA polymerases and reverse transcriptases in a K^+-dependent manner (*21*). The K^+-dependent block to DNA polymerase occurs only on DNA sequences containing stretches of guanine residues and is used as a selective and sensitive indicator of the formation of G-quadruplex structures (*36*). We have adapted this assay to further demonstrate the stabilization of G-quadruplex DNA by small molecules (*38*). In this assay PIPER does not cause general polymerase inhibition at the concentrations tested; however, addition of the ligand to the reaction mixture causes a sequence-specific polymerase arrest (Figure 6B) immediately before the G-quadruplex site. At a 10 μM drug concentration, polymerase arrest is so strong that full-length product is barely detected. Our results suggest that the ligand-stabilized G-quadruplex is a formidable obstacle for the polymerase reaction. Together with the high specificity of binding to

the G-quadruplex, this makes PIPER an interesting lead candidate for the study of the role of G-quadruplexes *in vivo* and suggests that it is not necessarily limited to telomerase inhibition.

Telomerase is an attractive target for cancer chemotherapy (*13*, *37*), but the presence of non-telomerase mechanisms for telomere length maintenance in some human cancer cells (*38*) can undermine its clinical validity. Alternative approaches for affecting the telomere length may be necessary. In this respect, the ability of G-quadruplex-stabilizing compounds to block polymerase synthesis on guanine-rich sequences (the human telomere is a primary example of such a sequence) may prove these compounds to be of value as antiproliferative drugs.

ACKNOWLEDGMENT

We acknowledge Dr. Daniel D. Von Hoff for his leadership of the NCDDG group, Dr. Daekyu Sun for the use of his telomerase assay, and David M. Bishop for proofreading, editing, and preparing the final version of the manuscript. Oleg Fedoroff is grateful to Dr. Qingping Zeng for his help with the synthesis of PIPER.

SUPPORTING INFORMATION AVAILABLE

Chemical shift assignments of the 1:1 $[dTAGGGTTA]_4$−PIPER and 2:1 $[dTTAGGG]_4$−PIPER complexes at 50 °C (2 pages). Ordering information is given on any current masthead page.

REFERENCES

1. Blackburn, E. H. (1994) *Cell 77*, 621−623.
2. Zakian, V. A. (1995) *Science 270*, 1601−1607.
3. Blackburn, E. H., and Greider, C. W., Eds. (1995) *Telomeres*, Cold Spring Harbor Press, New York.
4. Makarov, V. L., Hirose, Y., and Langmore, J. P. (1997) *Cell 88*, 657−666.
5. Wright, W. E., Tesmer, V. M., Huffman, K. E., Levene, S. D., and Shay, J. W. (1997) *Genes Dev. 11*, 2801−2809.
6. De Lange, T. (1994) *Proc. Natl. Acad. Sci. U.S.A. 91*, 2882−2885.
7. Harley, C. B., and Villeponteau, B. (1995) *Curr. Opin. Genet. Dev. 5*, 249−255.
8. Bodnar, A. G., Ouellette, M., Frolkis, M., Holt, S. E., Chiu, C.-P., Morin, G. B., Harley, C. B., Shay, J. W., Lichtsteiner, S., and Wright, W. E. (1998) *Science 279*, 349−352.
9. Lingner, J., Hughes, T. R., Shevchenko, A., Mann, M., Lundblad, V., and Cech, T. R. (1997) *Science 276*, 561−567.
10. Nakamura, T. M., Morin, G. B., Chapman, K. B., Weinrich, S. L., Andrews, W. H., Lingner, J., Harley, C. B., and Cech, T. R. (1997) *Science 277*, 955−959.
11. Feng, J., Funk, W. D., Wang, S. S., Weinrich, S. L., Avillon, A. A., Chiu, C. P., Adams, R. R., Chang, E., Allsop, R. C., and Yu, J. (1995) *Science 269*, 1236−1241.
12. Rhyu, M. S. (1995) *J. Natl. Cancer Inst. 87*, 884−894.
13. Parkinson, E. K. (1996) *Br. J. Cancer 73*, 1−4.
14. Sun, D., Thompson, B., Cathers, B. E., Salazar, M., Kerwin, S. M., Trent, J. O., Jenkins, T. C., Neidle, S., and Hurley, L. H. (1997) *J. Med. Chem. 40*, 2113−2116.
15. Norton, J. C., Piatyszek, M. A., Woodbring, E. W., Shay, J. W., and Corey, D. R. (1996) *Nat. Biotechnol. 14*, 615−619.
16. Wang, Y., and Patel, D. J. (1992) *Biochemistry 31*, 8112−8119.
17. Wang, Y., and Patel, D. J. (1993) *Structure 1*, 263−282.
18. Balagurumoorthy, P., and Brahmachari, S. K. (1994) *J. Biol. Chem. 269*, 21858−21869.
19. Zahler, A. M., Williamson, J. R., Cech, T., and Prescott, D. M. (1991) *Nature 350*, 718−720.
20. Daniels, G. A., and Lieber, M. R. (1995) *Nucleic Acids Res. 23*, 5006−5011.
21. Woodford, K. J., Howell, R. M., and Usdin, K. (1994) *J. Biol. Chem. 269*, 27029−27035.
22. Catasti, P., Chen, X., Moyzis, R. K., Bradbury, E. M., and Gupta, G. (1996) *J. Mol. Biol. 264*, 534−545.
23. Simonsson, T., Pecinka, P., and Kubista, M. (1998) *Nucleic Acids Res. 26*, 1167−1172.
24. Wellinger, R. J., and Sen, D. (1997) *Eur. J. Cancer 33*, 735−749.
25. Chung, I. K., Mehta, V. B., Spitzner, J. R., and Muller, M. T. (1992) *Nucleic Acids Res. 20*, 1973−1977.
26. Liu, Z., and Gilbert, W. (1994) *Cell 77*, 1083−1092.
27. Bashkirov, V. I., Scherthan, H., Solinger, J. A., Buerstedde, J.-M., and Heyer, W.-D. (1997) *J. Cell Biol. 136*, 761−773.
28. Harrington, C., Lan, Y., and Akman, S. A. (1997) *J. Biol. Chem. 272*, 24631−24636.
29. Guo, Q., Lu, M., Marky, L. A., and Kallenbach, N. R. (1992) *Biochemistry 31*, 2451−2455.
30. Chen, Q., Kuntz, I. D., and Shafer, R. H. (1996) *Proc. Natl. Acad. Sci. U.S.A. 93*, 2635−2639.
31. Anantha, N. V., Azam, M., and Sheardy, R. D. (1998) *Biochemistry 37*, 2709−2714.
32. Wheelhouse, R. T., Sun, D., Han, H., Han, F. X., and Hurley, L. H. (1998) *J. Am. Chem. Soc. 120*, 3261−3262.
33. Liu, Z.-R., and Rill, R. L. (1996) *Anal. Biochem. 236*, 139−145.
34. Rodger, A., and Norden, B. (1997) *Circular Dichroism and Linear Dichroism*, Oxford University Press, New York.
35. Lyng, R., Rodger, A., and Norden, B. (1991) *Biopolymers 31*, 1709−1720.
36. Weitzman, M. N., Woodford, K. J., and Usdin, K. (1996) *J. Biol. Chem. 271*, 20958−20964.
37. Lee, H.-W., Blasco, M. A., Gottlieb, G. J., Horner, J. W., II, Greider, C. W., and DePinho, R. A. (1998) *Nature 392*, 569−574.
38. Bryan, T. M., Englezou, A., Dalla-Pozza, L., Dunham, M. A., and Reddel, R. R. (1997) *Nat. Med. 3*, 1271−1274.
39. Feigon, J., Koshlap, K. M., and Smith, F. W. (1995) *Methods Enzymol. 261*, 225−255.
40. Laughlan, G., Murchie, A. I. H., Norman, D. G., Moore, M. H., Moody, P. C. E., Lilley, D. M. J., and Luisi, B. (1994) *Science 265*, 520−524.

BI981330N